

Supporting information

Sorption and redox speciation of plutonium at the illite surface under highly saline conditions

Rémi Marsac^{a,b}, Nidhu lal Banik^{a,c}, Johannes Lützenkirchen^{a,*}, Alexandre Diascorn^{a,d}, Kerstin Bender^a, Christian Michael Marquardt^a, Horst Geckeis^a

Address:

^a Institut für Nukleare Entsorgung, Karlsruhe Institute of Technology, P.O. Box 3640, D-76021 Karlsruhe, Germany, Tel +4972160822420; Fax: +4972160823927

Present addresses:

^b Ecole Nationale Supérieure de Chimie de Rennes, UMR CNRS 6226, 11 Allée de Beaulieu, F-35708 Rennes Cedex 7, France.

^c Institute for Transuranium Elements, European Commission P.O.Box 2340, D-76125 Karlsruhe

^d Groupe d'Etudes Atomiques (GEA), Ecole des Applications Militaires de l'Energie Atomique (EAMEA). BCRM Cherbourg, CC19 50115 Cherbourg-Octeville Cedex, France

*Corresponding author:

E-mail adresse: johannes.luetzenkirchen@kit.edu

Phone + 49 721 608-24023 / Fax + 49 721 608-23927

1. Thermodynamic calculations

Table S1. Reactions considered relevant for the calculation of Pu sorption and speciation in the present study. Thermodynamic constants are taken from the NEA-TDB [1] and refer to the value at infinite dilution. In case of gaps in the available database for Pu, data for analogues are used (i.e. Eu(III), Np(IV), Np(V) and U(VI) for the respective Pu redox states). Formation constants for PuOH^{2+} and $\text{Pu(OH)}_{4(\text{aq})}$ are taken from Eu(III) and Np(IV) to ensure the consistency between aqueous speciation and surface complexation modeling although available for Pu. This is done to avoid additional corrections of the literature parameters for the 2 SPNE SC/CE model. It should be noted, however, that differences in constants are not significant.

	Reaction	Log K		
Redox	$\text{PuO}_2^{2+} + \text{e}^- = \text{PuO}_2^+$	15.82		
	$\text{PuO}_2^{2+} + 4 \text{H}^+ + 2 \text{e}^- = \text{Pu}^{4+} + 2 \text{H}_2\text{O}$	33.27		
	$\text{PuO}_2^+ + 4 \text{H}^+ + \text{e}^- = \text{Pu}^{4+} + 2 \text{H}_2\text{O}$	17.45		
	$\text{Pu}^{4+} + \text{e}^- = \text{Pu}^{3+}$	17.69		
	Reaction	Available for Pu	Value used	Analogue
Hydrolysis	$\text{AnO}_2^{2+} + \text{H}_2\text{O} = \text{AnO}_2\text{OH}^+ + \text{H}^+$	-5.50	-5.50	
	$\text{AnO}_2^{2+} + 2 \text{H}_2\text{O} = \text{AnO}_2(\text{OH})_2 + 2 \text{H}^+$	-13.20	-13.20	
	$\text{AnO}_2^{2+} + 3 \text{H}_2\text{O} = \text{AnO}_2(\text{OH})_3^- + 3 \text{H}^+$		-20.25	U(VI)
	$\text{AnO}_2^+ + \text{H}_2\text{O} = \text{AnO}_2\text{OH} + \text{H}^+$		-11.30	Np(V)
	$\text{An}^{4+} + \text{H}_2\text{O} = \text{AnOH}^{3+} + \text{H}^+$	0.60	0.60	
	$\text{An}^{4+} + 2 \text{H}_2\text{O} = \text{An}(\text{OH})_2^{2+} + 2 \text{H}^+$	0.60	0.60	
	$\text{An}^{4+} + 3 \text{H}_2\text{O} = \text{An}(\text{OH})_3^+ + 3 \text{H}^+$	-2.30	-2.30	
	$\text{An}^{4+} + 4 \text{H}_2\text{O} = \text{An}(\text{OH})_4 + 4 \text{H}^+$	-8.50	-8.30	Np(IV)
	$\text{An}^{3+} + \text{H}_2\text{O} = \text{AnOH}^{2+} + \text{H}^+$	-6.90	-7.20	Am/Eu(III)
	$\text{An}^{3+} + 2 \text{H}_2\text{O} = \text{An}(\text{OH})_2^+ + 2 \text{H}^+$		-15.10	Am/Eu(III)
	$\text{An}^{3+} + 3 \text{H}_2\text{O} = \text{An}(\text{OH})_3 + 3 \text{H}^+$		-26.20	Am/Eu(III)
Chloride	$\text{AnO}_2^{2+} + \text{Cl}^- = \text{AnO}_2\text{Cl}^+$	0.23	0.23	
	$\text{AnO}_2^{2+} + 2 \text{Cl}^- = \text{AnO}_2\text{Cl}_2$	-1.15	-1.15	
	$\text{An}^{4+} + \text{Cl}^- = \text{AnCl}^{3+}$	1.80	1.80	
	$\text{An}^{3+} + \text{Cl}^- = \text{AnCl}^{2+}$		0.24	Am/Eu(III)
	$\text{An}^{3+} + 2 \text{Cl}^- = \text{AnCl}_2^+$		-0.74	Am/Eu(III)

Table S2. Surface complexation and cation exchange parameters (log K values) for the 2 SPNE SC/CE model are taken from the literature [2-4]. Source is given for each constant between brackets. The surface complexing site density is $[\equiv S]_{\text{tot}} = 2 \times 10^{-3}$ mol/kg.² The cation exchange capacity is $[X]_{\text{tot}} = 0.225$ eq/kg.² “na” refers to non-available values. Only the relevant reactions and constants for the present calculations are tabulated. According to our calculations, errors on each log K values for Pu/Eu in the 2 SPNE SC/CE model approximately equal the error on experimental log R_d values (i.e. ± 0.3 log unit, as considered in [3, 4]) because model parameters are weakly correlated.

	Reaction	Log K value
Surface	$\equiv\text{SOH} + \text{H}^+ = \equiv\text{SOH}_2^+$	4.00 [2]
	$\equiv\text{SOH} = \equiv\text{SO}^- + \text{H}^+$	-6.20 [2]
	$\equiv\text{SOH} + \text{Pu}^{4+} = \equiv\text{SO-Pu}^{3+} + \text{H}^+$	na
	$\equiv\text{SOH} + \text{Pu}^{4+} + \text{H}_2\text{O} = \equiv\text{SO-PuOH}^{2+} + 2 \text{ H}^+$	9.9 [3]
	$\equiv\text{SOH} + \text{Pu}^{4+} + 2 \text{ H}_2\text{O} = \equiv\text{SO-Pu(OH)}_2^+ + 3 \text{ H}^+$	5.9 [3]
	$\equiv\text{SOH} + \text{Pu}^{4+} + 3 \text{ H}_2\text{O} = \equiv\text{SO-Pu(OH)}_3^- + 4 \text{ H}^+$	0.1 [3]
	$\equiv\text{SOH} + \text{Pu}^{4+} + 4 \text{ H}_2\text{O} = \equiv\text{SO-Pu(OH)}_4^- + 5 \text{ H}^+$	-6.4 [3]
	$\equiv\text{SOH} + \text{Pu}^{3+} = \equiv\text{SO-Pu}^{2+} + \text{H}^+$	3.1 [4]
	$\equiv\text{SOH} + \text{Pu}^{3+} + \text{H}_2\text{O} = \equiv\text{SO-PuOH}^+ + 2 \text{ H}^+$	-4.4 [4]
Exchange	$3 \text{ X-Na} + \text{Pu}^{3+} = \text{X}_3\text{-Pu} + 3 \text{ Na}^+$	1.9 [4]
	$4 \text{ X-Na} + \text{Pu}^{4+} = \text{X}_4\text{-Pu} + 4 \text{ Na}^+$	na

Table S3. SIT parameters ($\varepsilon(i,k)$) used in the present study, taken from the NEA-TDB [1] for Pu or the corresponding analogue (as in Table S1). “na” refers to non-available values (set equal to 0).

i	k	$\varepsilon(i,k)$
H ⁺	Cl ⁻	0.12
Na ⁺	Cl ⁻	0.03
Na ⁺	OH ⁻	0.04
PuO ₂ ²⁺	Cl ⁻	0.22
PuO ₂ OH ⁺	Cl ⁻	na
PuO ₂ (OH) ₃ ⁻	Na ⁺	-0.09
PuO ₂ Cl ⁺	Cl ⁻	0.22
PuO ₂ ⁺	Cl ⁻	0.09
Pu ⁴⁺	Cl ⁻	0.40
PuOH ³⁺	Cl ⁻	0.20
Pu(OH) ₂ ²⁺	Cl ⁻	0.10
Pu(OH) ₃ ⁺	Cl ⁻	0.05
PuCl ³⁺	Cl ⁻	0.62
Pu ⁺³	Cl ⁻	0.23
PuOH ²⁺	Cl ⁻	-0.04
Pu(OH) ₂ ⁺	Cl ⁻	-0.06
Pu(OH) ₃	Cl ⁻	0.00
Pu(OH) ₃	Na ⁺	-0.17
PuCl ²⁺	Cl ⁻	0.191
PuCl ₂ ⁺	Cl ⁻	0.129

2. Predominance diagrams

Predominance diagrams for dissolved Pu are constructed for $m_{NaCl} = 0.1, 1$ and 3.2 m using PhreePlot [5] and the database given above. Only the prevalent redox state is shown, i.e. the various aqueous species for a given redox state do not appear. Fig. S1a shows the diagrams for $m_{NaCl} = 0.1, 1$ and 3.2 m using the pH-scale (i.e. the activity of the proton, a_{H^+}). In this case, the borderlines shift with m_{NaCl} only because of the variation in the activity coefficients for the dissolved species. Fig. S1b shows the same diagrams on the pH_m -scale (i.e. the molality of the proton, $[H^+]$). In Fig. S1b, the borderlines additionally shift with m_{NaCl} because of the change in the activity coefficients of H^+ , which can also be seen in the “ $H_{2(g)} > 1\text{ atm}$ ” and “ $O_{2(g)} > 0.2\text{ atm}$ ” lines. As stated in the article, these variations in the stability field of the different Pu redox states are small compared to the experimental uncertainties of pe.

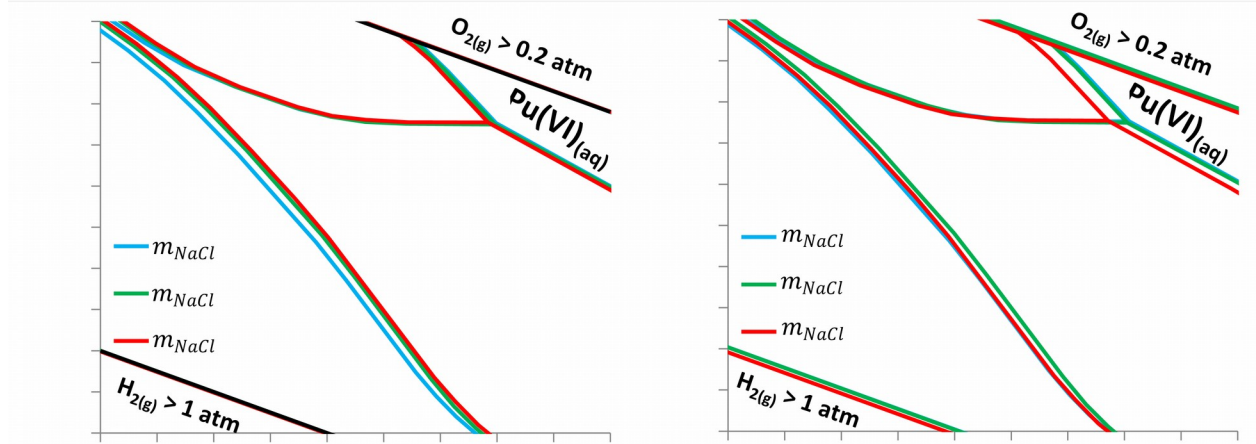


Fig. S1. Predominance diagrams for dissolved Pu in $m_{NaCl} = 0.1, 1$ and 3.2 m plotted on (a) the pH-scale and (b) the pH_m -scale.

3. Experimental results

Table S4. Experimental Eu-illite sorption data for $m_{NaCl} = 0.1, 0.9$ and 3.9 m ($[Eu]_{tot} = 3 \times 10^{-9}\text{ M}$, 2 g L^{-1} of illite, Ar atmosphere, 1 week equilibration time).

m_{NaCl}	pH _m	$\log R_d (\text{L kg}^{-1})$
0.1	8.8	5.8
	8.2	5.4
	7.7	5.6
	7.1	6.2
	6.8	5.5
	5.9	5.4
	5.4	4.9
	5.0	4.1
	4.6	3.6
	4.1	3.3
0.9	3.6	3.2
	8.8	5.9
	8.2	5.6
	7.8	5.7
	7.2	5.7
	6.9	5.2
	6.0	5.0
	5.5	4.1
	5.0	3.7
	4.6	2.7
0.9	4.2	2.0
	3.6	1.8
	8.8	5.4
	8.3	5.8
	7.8	5.6
	7.3	5.8
	6.8	5.2
	6.1	4.5
	5.5	3.9
	5.1	3.4
3.9	4.7	2.5
	4.2	1.7
	3.6	1.5

Table S5. Experimental Pu-illite sorption data for $m_{NaCl} = 1$ and 3.2 m (2 g L⁻¹ of illite, Ar atmosphere, 1 year equilibration time).

pH _m	m_{NaCl}	[Pu] _{tot} (M)	pe	Log [Pu] _{aq} (M)	Log R _d (L kg ⁻¹)
4.4	1.0	3×10^{-9}	7.0	-10.2	4.4
4.4	1.0	1×10^{-8}	7.0	-9.2	3.9
4.5	1.0	8×10^{-9}	6.9	-9.8	4.4
4.6	1.0	5×10^{-10}	7.4	-11.4	4.8
4.7	1.0	8×10^{-10}	7.2	-11.1	4.7
4.7	1.0	8×10^{-11}	8.0	-12.1	4.7
6.7	1.0	9×10^{-9}	5.0	-10.7	4.9
6.8	1.0	8×10^{-10}	4.8	-12.2	5.8
6.8	1.0	8×10^{-11}	5.0	-12.6	5.2
6.8	1.0	5×10^{-10}	4.9	-12.1	5.5
9.1	1.0	3×10^{-9}	5.1	-11.1	5.2
9.1	1.0	5×10^{-10}	3.5	-12.3	5.7
9.2	1.0	8×10^{-9}	4.9	-11.1	5.7
9.3	1.0	1×10^{-7}	4.6	-9.6	5.3
9.6	1.0	8×10^{-10}	3.2	-12.2	5.8
3.6	3.2	8×10^{-11}	5.7	-10.3	2.5
4.3	3.2	8×10^{-11}	6.0	-10.7	3.2
4.9	3.2	1×10^{-8}	5.5	-9.0	3.6
4.9	3.2	8×10^{-9}	5.7	-9.2	3.7
5.0	3.2	3×10^{-9}	5.7	-10.0	4.2
5.1	3.2	8×10^{-10}	6.4	-11.1	4.7
5.4	3.2	5×10^{-10}	6.7	-11.2	4.6
6.1	3.2	8×10^{-11}	5.2	-12.5	5.1
6.3	3.2	8×10^{-11}	5.1	-12.5	5.1
6.6	3.2	8×10^{-11}	5.0	-12.5	5.1
6.9	3.2	8×10^{-11}	5.2	-13.0	5.6
6.9	3.2	1×10^{-8}	6.5	-10.1	4.8
7.1	3.2	8×10^{-9}	6.5	-10.3	4.9
7.1	3.2	5×10^{-10}	5.0	-12.0	5.4
7.1	3.2	8×10^{-10}	5.0	-11.8	5.4
7.1	3.2	3×10^{-9}	6.6	-11.0	5.2
10.0	3.2	5×10^{-10}	4.6	-11.9	5.3
10.0	3.2	1×10^{-8}	4.5	-10.8	5.5
10.1	3.2	8×10^{-9}	4.3	-10.8	5.4
10.1	3.2	8×10^{-10}	4.4	-12.3	5.9
10.2	3.2	3×10^{-9}	4.4	-11.1	5.3
10.2	3.2	1×10^{-8}	3.6	-9.8	5.5

References:

- [1] R. Guillaumont, Th. Fanghänel, J. Fuger, I. Grenthe, V. Neck, D. A. Palmer, M. H. Rand, Update on the Chemical Thermodynamics of Uranium, Neptunium, Plutonium, Americium and Technetium; Elsevier: Amsterdam, 2003.
- [2] M. H. Bradbury, B. Baeyens, Geochim. Cosmochim. Acta, 73 (2009) 1004.
- [3] N. L. Banik, R. Marsac, J. Lützenkirchen, A. Diascorn, C. M. Marquardt, H. Geckeis, Environ. Sci. Technol., 50 (2016) 2092.
- [4] M. H. Bradbury, B. Baeyens, H. Geckeis, T. Rabung, Geochim. Cosmochim. Acta, 69 (2005) 5403.
- [5] D. G. Kinniburgh, D. M. Cooper, *PhreePlot: Creating graphical output with PHREEQC*, 2009. <http://www.phreeplot.org>